

Provided for non-commercial research and education use.
Not for reproduction, distribution or commercial use.

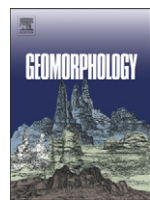


This article appeared in a journal published by Elsevier. The attached copy is furnished to the author for internal non-commercial research and education use, including for instruction at the authors institution and sharing with colleagues.

Other uses, including reproduction and distribution, or selling or licensing copies, or posting to personal, institutional or third party websites are prohibited.

In most cases authors are permitted to post their version of the article (e.g. in Word or Tex form) to their personal website or institutional repository. Authors requiring further information regarding Elsevier's archiving and manuscript policies are encouraged to visit:

<http://www.elsevier.com/copyright>



Scientific visualization of landscapes and landforms

Helena Mitasova ^{a,*}, Russell S. Harmon ^b, Katherine J. Weaver ^a, Nathan J. Lyons ^a, Margery F. Overton ^c

^a Department of Marine, Earth and Atmospheric Sciences, North Carolina State University, Raleigh, NC 27695, USA

^b Environmental Sciences Division, Army Research Office, U.S. Army Research Laboratory, Durham, North Carolina, 27703, USA

^c Department of Civil, Construction, and Environmental Engineering, North Carolina State University Raleigh, NC 27695, USA

ARTICLE INFO

Article history:

Received 25 March 2010

Received in revised form 7 September 2010

Accepted 8 September 2010

Available online 13 June 2011

Keywords:

Relief shading

DEM time series

LiDAR

Tangible geospatial modeling

GRASS GIS

ABSTRACT

Scientific visualization of geospatial data provides highly effective tools for analysis and communication of information about the land surface and its features, properties, and temporal evolution. Whereas single-surface visualization of landscapes is now routinely used in presentation of Earth surface data, interactive 3D visualization based upon multiple elevation surfaces and cutting planes is gaining recognition as a powerful tool for analyzing landscape structure based on multiple return Light Detection and Ranging (LiDAR) data. This approach also provides valuable insights into land surface changes captured by multi-temporal elevation models. Thus, animations using 2D images and 3D views are becoming essential for communicating results of landscape monitoring and computer simulations of Earth processes. Multiple surfaces and 3D animations are also used to introduce novel concepts for visual analysis of terrain models derived from time-series of LiDAR data using multi-year core and envelope surfaces. Analysis of terrain evolution using voxel models and visualization of contour evolution using isosurfaces has potential for unique insights into geometric properties of rapidly evolving coastal landscapes. In addition to visualization on desktop computers, the coupling of GIS with new types of graphics hardware systems provides opportunities for cutting-edge applications of visualization for geomorphological research. These systems include tangible environments that facilitate intuitive 3D perception, interaction and collaboration. Application of the presented visualization techniques as supporting tools for analyses of landform evolution using airborne LiDAR data and open source geospatial software is illustrated by two case studies from North Carolina, USA.

© 2011 Elsevier B.V. All rights reserved.

1. Introduction

Scientific visualization provides a means for effective analysis and communication of complex information that may be otherwise difficult to explain. This particularly applies to geomorphology, where 3D spatial patterns and relationships are critical for depicting landscape features and understanding observed or modeled phenomena. Online access to massive volumes of geospatial data, coupled with fast graphics and computational power, has expanded the use of visualization in Earth sciences and education. The data acquired by modern mapping technologies established a new foundation for landform analysis at unprecedented levels of detail and spatial extent (Bellian et al., 2005). Airborne Light Detection and Ranging (LiDAR) and Interferometric Synthetic Aperture Radar (IfSARE) have dramatically changed the level of detail captured in digital elevation models (DEMs,) including public statewide data at 3 m–10 m resolutions (Gesch et al., 2009) and regional data at 0.3 m–1.0 m resolutions (NOAA Coastal Services Center, 2010). The spatial extent of public elevation data at resolutions 90 m and better have increased to near-

global coverage, starting with the Shuttle Radar Topographic Mission (SRTM) in the year 2000 (Rabus et al., 2003). Field scale data are now routinely acquired at 0.10 m resolutions and higher using ground based laser scanning (Heritage and Hetherington, 2007).

DEMs generated from these new sensing technologies have different properties than traditional DEMs derived from topographic map contours or older photogrammetric data (Mitasova et al., 2005a), and consequently pose challenges for processing, analysis, and visualization. High spatial and temporal resolutions in the case of LiDAR data or the vastly expanded, almost global coverage of the SRTM-based elevation models and the ASTER Global Digital Elevation Model (Earth Remote Sensing Data Analysis Center, 2009) lead to massive data sets that cannot be visualized on the computer screen at full resolutions, therefore, fast zoom-in and zoom-out capabilities are essential. Hierarchical data structures, based on pyramids, are used to view such data, especially in online applications (Tanimoto and Pavlidis, 1975; Lowe, 2004; Whitmeyer et al., 2008). Moreover, these elevation data are often noisy and include extensive detail that may obstruct landforms, so further processing may be needed to create a model with an appropriate level of detail for a given application (Mitasova et al., 2005b). Landform visualization from multiple return LiDAR point clouds in vegetated or developed areas requires filtering of points to remove above ground surface clutter (Sithole and Vosselman, 2004) and provide bare-Earth

* Corresponding author. Tel.: +1 919 513 1327.

E-mail addresses: hmitaso@unity.ncsu.edu (H. Mitasova), russell.harmon@us.army.mil (R.S. Harmon), overton@ncsu.edu (M.F. Overton).

elevations. At the same time, the above ground data provide valuable information about the structure of vegetation and anthropogenic features that are important for studies of landscape evolution. In addition to static terrain representations, the high efficiency of current technology facilitates repeated surveys of rapidly changing landscapes making elevation time series animations indispensable for analyzing and communicating land surface dynamics.

Scientific visualization of geospatial data has its foundation in cartography and computer graphics. Although most of the fundamental methods have not changed over the past two decades (e.g., contours and relief shading for elevation data) many advanced, interactive tools have become more accessible and easier to use. Buckley et al. (2004) provides a comprehensive overview of cartographic methods for topographic data representation, ranging from traditional cartographic techniques such as contouring and hypsometric tinting to computer generated relief shading and terrain visualization in 3D perspective. Whereas this extensive review is focused on mountain geomorphology, most of the methods are general and are applicable to other types of landscapes. More recent research on landscape visualization builds upon these traditional techniques by taking advantage of high resolution elevation data, faster computer graphics and multi-modal human-computer interaction.

Multiple return LiDAR technology, supporting highly efficient repeated elevation mapping over large regions, provides a unique opportunity to move beyond the study of terrain as a bare Earth, relatively stable surface towards its representation as a dynamic 3D layer. This layer can be investigated as a set of dynamic, interacting surfaces representing bare Earth, vegetation canopy, understory plant cover, water surface, anthropogenic features, and anthropogenic structures. The objective in this paper is to explore this concept and illustrate applications of visualization coupled with GIS to investigate short term terrain change and its impacts. Specifically, we focus on evolving landscapes and visualization of features related to recent change and short-term (decadal) dynamics captured by laser scanning technologies. All presented applications and visualizations are performed using open source GRASS GIS tools (Neteler and Mitasova, 2008).

In the first section that follows, we review advances in visualization technology and systems that were developed largely in response to the need for display, exploration and navigation through massive elevation data sets that became available over the past decade. Then, we describe specific techniques for visualization of landscapes using elevation models derived from multiple return LiDAR point clouds, followed by explanation of innovative concepts for visualizing landscape dynamics using multiple surfaces, voxel models and animations. The exploratory Tangible Geospatial Modeling System (TanGeoMS) is introduced as an example of multi-modal approach that has been specifically designed for interactive investigation and visualization of terrain change impacts on topographic parameters and landscape processes. Finally, the techniques presented are combined in case studies that use visualization to assist investigation of landforms and recent landform evolution in mountainous and coastal landscapes.

2. Advances in visualization technology and systems

Modern mapping technologies and efficient, Internet-based distribution of geospatial data have driven the development of software and hardware solutions that facilitate visual exploration of massive elevation data sets. Powerful graphics cards and hierarchical data structures now support fast zooming capabilities and fly-through applications, providing fast previews of the available data. Tiled displays, composed of many screens and supporting resolutions of more than 100 million pixels, provide means for display of elevation data as 2D images or in 3D perspective at high resolutions for large areas (Sorokine, 2007; DeFanti et al., 2009).

To support in-depth perception of topography and its landforms, immersive technologies have been coupled with GIS in ways that are useful for geoscience research and education. For example, Geowall employs a single wall stereo projection to provide 3D immersion (Johnson et al., 2006) while Vision Dome displays create a fully immersive 360° projection with 180° field of view. Cave Automatic Virtual Environment (CAVE™), an immersive virtual reality system, projects images on 3–6 walls of a room-sized cube. This technology has allowed users to interact with 3D dynamic simulations of landscape processes such as surface water flow (Johnston, 1998), to explore 3D volume data such as the structure of detrital sedimentary rocks and fossil mats (Billen et al., 2008), and to visualize subsurface seismic data (Lin and Lofton, 1998). Whereas these systems allow users to explore large regions at high resolutions and immersion can provide field-scale experience, special facilities and expensive hardware are required. Emerging frameworks provide tools to integrate multi-temporal land surfaces with sub-surface volume data and visualize them in high-end immersive environments as well as through web mapping service (Baru et al., 2008), which makes the sophisticated multidimensional visualization of Earth science data sets available to researchers and educators without the specialized hardware.

The introduction of Virtual Globes, such as Google Earth or NASA WorldWind (Boschetti et al., 2008; Tuttle et al., 2008), has had the broadest impact on landscape visualization to date by providing elevation data combined with Earth imagery and easy to use navigation over the web. Originally, the Virtual Globe approach was developed for the general public, but over time it has become widely adopted by the scientific community and has stimulated innovation in methods to interactively present and share geoscience information. For example, the OpenTopography portal, supported by the National Science Foundation (NSF), provides browsing access to its vast repository of scientific LiDAR data through Google Earth relief shaded images (Prentice et al., 2009). Fault model visualization (Van Aalsburg et al., 2009) combines high resolution DEMs with active tectonic fault maps and earthquake hypocenters and creates a graphical output that can be visualized in Google Earth on desktop computers or in virtual environments such as CAVE or Geowall.

To further improve the interaction with virtual landscape models and associated geospatial data, traditional point-click-drag control with a computer mouse is being replaced by screen touch applications ranging from interactive maps on smart phones to large touch tables and screen displays used for collaboration and in media to display and manipulate geospatial data. Interscopic multi-touch surfaces (Schöning et al., 2009) allow users to interact with 3D topographic and urban data using hands and manually modify shapes of virtual volumes. Multi-modal interfaces for navigation through terrain add speech and gesture interaction and are considered important candidates for mobile, field, or ubiquitous applications (Krum et al., 2002). Multi-touch hand and foot gestures have been recently combined to create an intuitive 3D interface for interaction with geospatial data (Valkov et al., 2010).

Several new technologies extend visualization beyond the 2D displays and merge 3D scale models with imagery. Simple systems project GIS data over a solid 3D model (Coucelo et al., 2005). The technologically complex Terrain Table created the scale model dynamically using movable pins covered by a flexible plastic sheet (Directions Staff, 2004; Marshal, 2004; Defense Update, 2005). Although the detail represented by the pins was rather limited, high resolution imagery was projected over its surface to enhance the perception of landscape features.

Systems aimed at research applications go beyond data query and navigation by integrating the display of georeferenced data with geospatial analysis, simulations and modeling. Underkoffler and Ishii (1999) added movable tagged objects to the touch table and coupled it with simulation tools that responded to the movement of the objects in real time. For example, if the objects represented buildings

that were moved around by a user-architect, the system generated immediate feedback about changes in casted shadows or in the wind vector field. Illuminated Clay (Ratti et al., 2004; Mitasova et al., 2006) employed a flexible clay terrain model as a tangible interface that responded to the manually introduced changes in its form by projecting near real-time updates to the terrain parameters such as slope angle or profile.

Whereas the new hardware and software technology has greatly improved the visual perception and exploration of complex, massive elevation data, it still relies on a fast display of 3D perspective views, 2D shaded relief, 2D color maps, and isolines. In the following sections we discuss the core techniques for visualization of a single landscape surface and present extension of these techniques to support visual analysis of multiple return LiDAR data and time series of DEMs.

3. Visualization of single, multiple and dynamic elevation surfaces

Surface visualization, using a 2D shaded relief image or a 3D perspective view, fully integrated within most GIS and remote sensing software systems, has become a core tool for visual analysis of landscapes and landforms. In addition to the traditional single surface display, various techniques based on combination of multiple surfaces have become essential tools for visual analysis and communication of information from multiple return LiDAR data and time series of DEMs.

3.1. Visualization of a static, bare Earth surface

Relief shading (e.g. Horn, 1981) and illuminated surface visualization in 3D perspective are gradually replacing contours as means to represent and analyze elevation data, identify potential artifacts in DEMs, and make decisions about additional processing that may be needed for landform mapping. These techniques are capable of capturing subtle features that are often missed by the traditional contour representation and have become one of the preferred techniques for visualization of high resolution LiDAR-based DEMs.

Image representing relief shading is derived by computing the image intensity values as a function of illumination angle g (angle between the incoming light source ray and elevation surface normal):

$$\cos(g) = \cos(z)\cos(s) + \sin(z)\sin(s)\cos(a-o)$$

where z is light source altitude angle measured from zenith, s is elevation surface slope angle, a is light source azimuth and o is elevation surface aspect. Landscapes with relatively flat topography, such as plains or plateaus, require large z angle (low light source) to reveal shallow depressions, old channels and other types of subtle landforms, whereas features with steep slopes are sensitive to light source azimuth. Therefore, a high level of interaction that supports continuous control of light source zenith and azimuth is important for

the selection of effective lighting parameters. Multiple light sources can be used to reduce the negative effects of azimuth biasing that can diminish visibility of landscape features oriented parallel to the light source azimuth (Smith and Clark, 2005; Smith and Wise, 2007). For example, the visualization tool in GRASS GIS (Neteler and Mitasova, 2008, chapter 7.3) uses two light sources: a dim white light remains directly above the surface at all times and serves as a fill light, creating a component of illumination that is function of slope and is independent of azimuth. The position of the second light source is adjustable and controlled interactively by the user. When light is being adjusted, a sphere appears on the surface and is continuously redrawn to show the effects of lighting changes (Fig. 1). Neither light is directional, light is emitted equally in all directions from the light source.

Relief shading provides a 2D orthogonal view of the topography at a uniform scale and it is suitable for landform mapping using on-screen digitizing (Smith and Clark, 2005). For example, this approach has been identified as one of the most effective methods for identification of linear landforms from remotely sensed data if the single or multiple light source positions are properly selected (Smith and Wise, 2007). To highlight the mapped topographic features relief shading is often combined with topographic parameters such as slope and curvatures, or spatial statistics measures (Mitasova et al., 2005a; Smith and Clark, 2005).

Illuminated surface visualization in a 3D perspective view improves perception of relative elevation that can be interactively exaggerated to highlight even small landforms and anthropogenic features such as roads or bridges (Fig. 1). The images of perspective views have variable scales and are, therefore, rarely used for digitizing.

Draping of a color map over an elevation model is widely used to convey the relationship between the surface geometry and parameters derived from the DEM such as slope, aspect, curvatures, ridges, stream networks, or viewsheds. Color maps are also used to represent phenomena that are only partially controlled by topography such as land cover, soils and geology (Buckley et al., 2004). Histogram equalized color ramps employ a monotonic, non-linear mapping which assigns the color values to grid cells to achieve uniform distribution of colors. These color ramps are effective for highlighting topographic features in regions with uneven distribution of elevation (the state of North Carolina is a typical example, Fig. 2a). Logarithmic color ramps are often needed to visualize flow accumulation patterns or other phenomena where the values range over several magnitudes (Fig. 2b).

In addition to the color maps, 2D vector features, such as lines, points, or area polygons, can be draped over the illuminated elevation surface to provide baseline information (streams, roads, etc.) or geomorphologic and geologic features (e.g., landform boundaries, fault lines). Surfaces can be also combined with 3D vector data, for example to explore the relation of the multiple return point cloud to

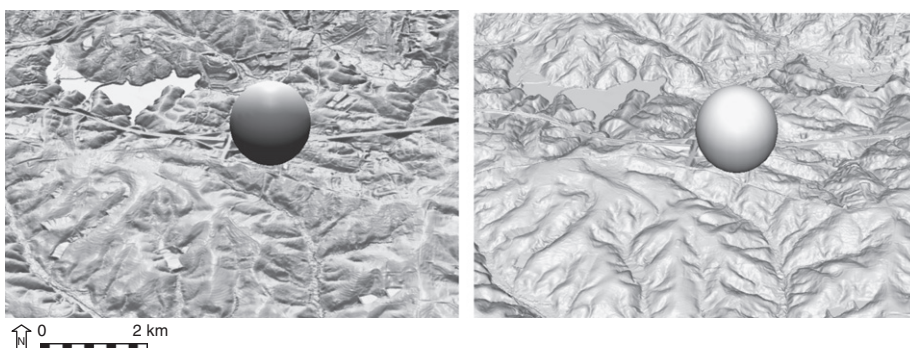


Fig. 1. Surface visualization with interactive light adjustment: simple geometrical object such as a sphere is used to guide the light source position. The surface is displayed with 3-times vertical exaggeration.

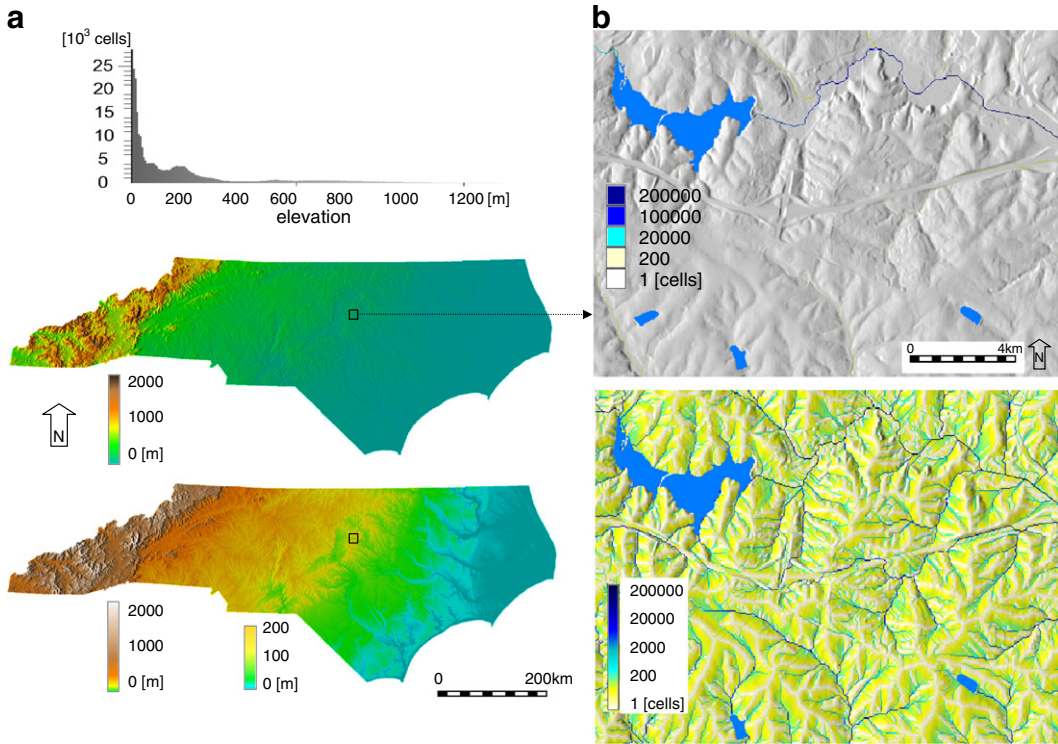


Fig. 2. Adjusting color ramps to extract topographic features: (a) comparison of North Carolina DEM displayed with equal interval and histogram equalized color ramps, the latter highlights the subtle topography of North Carolina coastal plain; (b) flow accumulation derived from a 10 m resolution DEM displayed over shaded relief with two different color ramps: equal interval (only the largest stream is visible) and logarithmic (detailed structure of stream network can be identified).

bare ground surface (Fig. 3a) or to represent structures such as buildings and bridges.

3.2. Multiple surface visualization and DEM time series

Multiple return LiDAR data capture the bare Earth surface along with the vegetation and structures, thus, mapping landscapes as a 3D layer rather than a single bivariate surface (Fig. 3a). Several types of surfaces can be extracted from LiDAR point clouds using point filtering algorithms (Sithole and Vosselman, 2004), including the bare Earth surface $z = F_b(x, y)$, elevation surface representing bare Earth with

vegetation canopy and structures $z = F_v(x, y)$, or a surface representing understory vegetation. Relation between F_b and F_v including structure of the canopy is then visualized using multiple surfaces (Fig. 3b).

Multiple surfaces are also widely used for analysis of topographic change and land surface evolution. In addition to surface overlays (e.g., Mitasova et al., 2005a), spatial patterns of terrain dynamics can be mapped and quantified using the concepts of *core* and *envelope* surfaces (Fig. 4) and *time of minimum* and *time of maximum* maps (Mitasova et al., 2009). Given a series of raster-based DEMs $z(i, j, t_k)$ acquired at time snapshots $t_k, k = 1, \dots, n$, it we define a *core surface* as

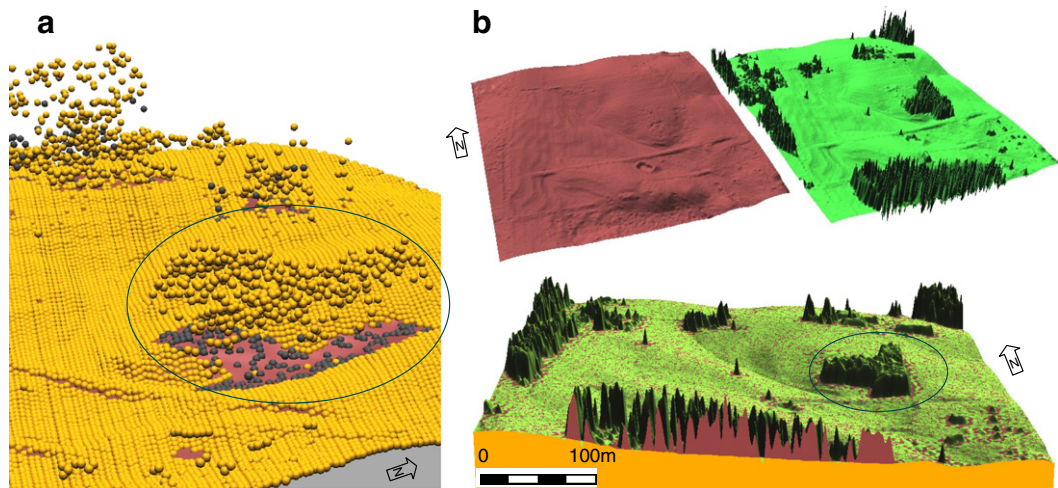


Fig. 3. Visualization based on multiple return LiDAR data: (a) point cloud; (b) bare Earth and first return surfaces side-by-side and overlaid with a crosssection. Image adapted from Neteler and Mitasova (2008).

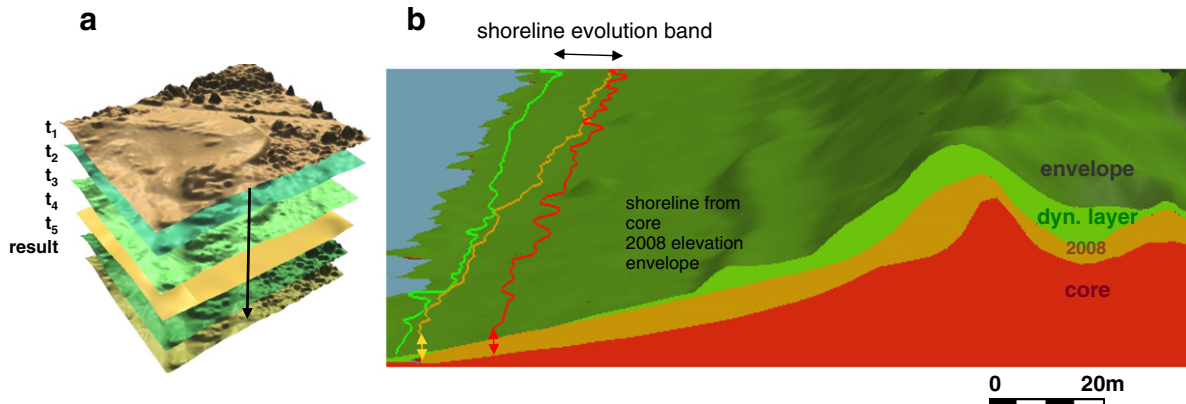


Fig. 4. Raster-based analysis of elevation time series: (a) principle, (b) relation between a dynamic layer defined by the core and envelope surfaces and shoreline band, extracted as mean high water level (MHWL) for beach-foredune system.

the minimum elevation and an *envelope surface* as the maximum elevation measured at each cell over the given time period (t_1, t_n) such that:

$$z_{\text{core}}(i,j) = \min_k z(i,j, t_k) \quad z_{\text{env}}(i,j) = \max_k z(i,j, t_k)$$

The core surface represents the boundary between a stable volume that has not moved during the entire study period and a *dynamic layer*. The envelope surface represents the outer boundary of the dynamic layer within which the terrain evolved during the given time period. Contours (elevation isolines) extracted from the core and envelope surfaces for the given elevation $z=c$ then define a *contour evolution band* area within which the given contour c evolved during the time period (t_1, t_n). In coastal studies, an emerging application of the contour evolution band concept is to extract isolines representing different shoreline positions through time and, thus, efficiently map the area of shoreline dynamics (Fig. 4b), a task that has been traditionally performed by manually digitizing an envelope from a time series of shorelines positions extracted from 2D imagery. Spatial patterns of time associated with the core and envelope surfaces are derived as raster maps that represent *time of minimum elevation* and *time of maximum elevation*:

$$t_{\max}(i,j) = t_k \text{ where } z(i,j, t_k) = z_{\text{env}}(i,j)$$

$$t_{\min}(i,j) = t_l \text{ where } z(i,j, t_l) = z_{\text{core}}(i,j)$$

where values in the time maps represent the index l or p for the relevant DEM in the time series and the actual date t_l or t_p is stored as an attribute (grid cell label).

The relationship between the core, envelope and an elevation surface, captured at a given time, is visualized using multiple surfaces with interactive cutting planes (Fig. 4). For example, position of a newly surveyed DEM within or outside the dynamic layer indicates whether the observed change is within the extent of n -year dynamic fluctuation or whether it creates a new minimum or maximum boundary. The dynamics of the actual elevation surface can be visualized by animations within the cross-sections or as a dynamic surface.

3.3. Animations and space-time domain volumes

Animations have become an indispensable tool for analysis, visualization and communication of landscape evolution based on monitoring data and modeling. Time series of landscape monitoring data acquired by remote sensing are now routinely viewed using 2D and 3D animations (Andrews et al., 2002; Buckley et al., 2004; Napieralski et al., 2007). Changing color maps draped over a 3D

perspective view of a static elevation surface or an evolving 3D surface are effective for analyzing and communicating the relationship between landforms and process dynamics, such as overland water flow or erosion and sediment transport (Mitas et al., 1997; Andrews et al., 2002; Luo et al., 2004). Dynamic surfaces have also been used to test and improve methods and algorithms for land surface modeling (Mitas et al., 1997).

Animating results of simulations is relatively straightforward because simulation tools usually provide adequate control over the time step and resolution of the output maps. Processing monitoring data for animations is more challenging because the time step or spatial coverage may not be adequate and robust multivariate interpolation becomes essential for filling the gaps in data (Mitasova et al., 1995). Sequences of raster maps computed by simulation tools, or by processing of monitoring data, are then animated using 2D images or as a movie representing dynamic surfaces generated by 3D visualization tools (Mitas et al., 1997).

The analysis, based on time series of DEMs, usually handles evolution over time as a series of discrete events. To apply the full power of analysis based on multivariate differential geometry land surface evolution can be represented as a trivariate function:

$$z = G(x,y,t)$$

where x, y is horizontal location, t is time and elevation z is the modeled variable. The function $G(x,y,t)$ is derived from a series of m point clouds $\{(x_i, y_i, z_i)\}, i=1, \dots, n_k, t_k, k=1, \dots, m$, where x, y, z are coordinates, n_k is number of points in the k -th point cloud and t_k is the time of the survey. We merge the data from all point clouds and re-organize them into a single point cloud $\{(x_i, y_i, t_i, z_i) | i=1, \dots, \sum n_k\}$ that is then interpolated into a voxel model (3D grid) using trivariate interpolation function (Fig. 5), in our case the regularized smoothing spline, with anisotropic tension applied in the time dimension (Mitasova et al., 1995). Oct-tree segmentation is used to support spatial interpolation of the large merged point cloud. Time resolution is selected to be close to the time interval of the surveys, although the approach is designed to handle irregular time intervals as well.

Evolution of a given contour $z=c$ is then visualized as a set of isosurfaces extracted from the voxel model. For example, shoreline evolution will be represented by the isosurface $z=z_{\text{MHW}}$, where z_{MHW} is mean high water elevation level. Visual analysis of space-time isosurface topology is useful for identification of specific surface evolution features. For example, if the extracted contour represents elevation close to a foredune ridge, "holes" in the isosurface represent temporal loss of elevation that has recovered typical for an overwash after which the dune was repaired or recovered (Fig. 6). Closed surfaces (spheroids) represent short term gain at the elevation level

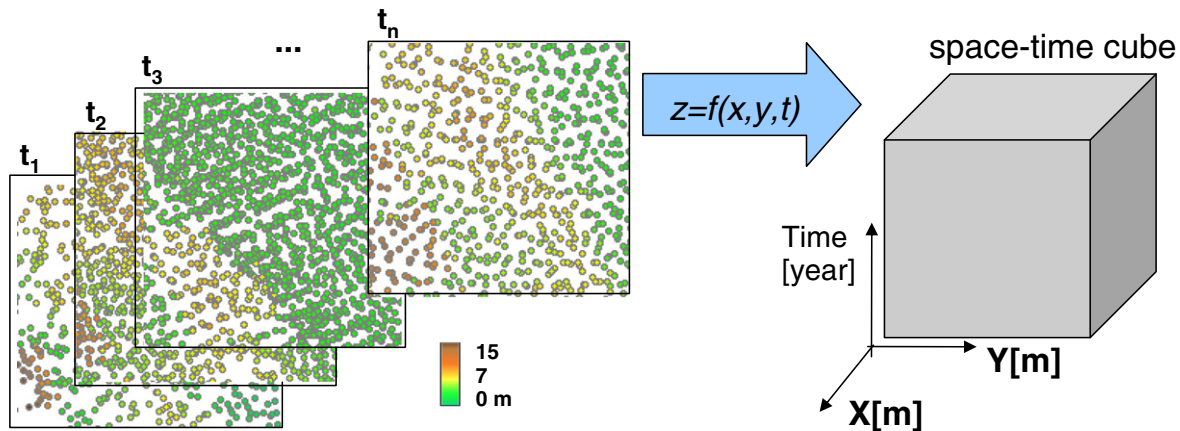


Fig. 5. Representation of terrain evolution using trivariate space–time function: merged time series of point clouds is interpolated into space–time voxel model.

examined. This visualization concept is similar to the space–time cube approach proposed for epidemiologic studies (Kraak and Madzudzo, 2007) or remote sensing meteorological data (Turdukulov et al., 2007).

3.4. Visualization of landform change impacts using Tangible Geospatial Modeling System

The previous sections focused on visualization of terrain state and dynamics as captured by surveys using virtual terrain models representing real-world topography. Many applications, especially in land use management, landscape design, military installation operational planning, or education exist, however, where modified terrain conditions and

their impact on landscape processes need to be evaluated, often in a collaborative setting. Although virtual models are excellent for analysis of real-world data they, have some limitations when introducing modifications in topography. On-screen editing of 3D models can be tedious and requires knowledge of editing software tools. Model translation through 2D display and indirect interaction using a mouse can hamper creativity and restrict collaboration. Professionals in creative disciplines, such as landscape architects or designers, use sketching to explore various design options and as a means for exchanging ideas. Similarly, scientific drawings convey alternative hypotheses about studied phenomena, and serve as a graphical aid to discuss concepts or propose solutions to a studied problem. Geodesign has been proposed as a method that “brings

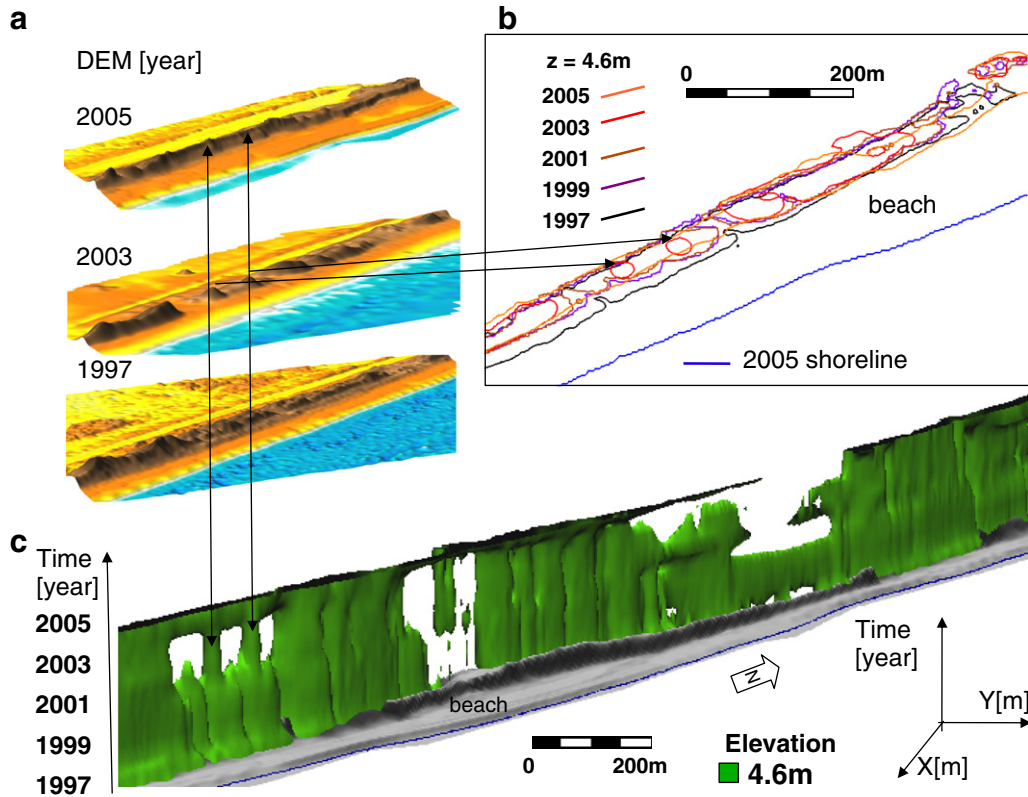


Fig. 6. Evolution of a foredune: (a) three snapshots from the DEM time series illustrating changes in the beach-foredune system, including an overwash in the year 2003, (b) evolution of a 4.6 m contour displayed as a set of overlapping lines, image is hard to read due to the complexity of changes in the dune morphology, (c) displayed as isosurface extracted from the voxel model, holes in the isosurface represent the dune overwash caused by the year 2003 hurricane, after which the dune was repaired (example from the Pea Island, North Carolina, see more details about this site in Mitasova et al., 2009).

geographic analysis into the design process, where initial design sketches are instantly vetted for suitability against a myriad of database layers describing a variety of physical and social factors for the spatial extent of the project" (Dangermond, 2009). Tangible interface for a virtual landscape model is an example of geodesign environment that provides users with creative freedom, an analogy to sketching in three dimensions, and combines it with scientific tools for geospatial analysis, providing rapid feedback that supports learning and decision making.

The Tangible Geospatial Modeling System (TanGeoMS, Tateosian et al., 2010) couples an indoor 3D laser scanner, projector and a flexible physical 3D model with a standard GIS (in our case GRASS, Neteler and Mitasova, 2008) to create a tangible interface for terrain data. The system configuration is flexible and additional projectors, 3D displays, or scanners can be added as needed (Fig. 7a). The 3D scale model (1:1200–1:3000 scales were tested) is constructed to have a soft plasticine surface that can be manually modified to create various landscape configurations by changing the surface geometry by hand (Fig. 7c). Surface depressions can be pushed-in to create ponds and stream channels, dams and levees can be added and the surface roughness can be modified to represent vegetation, disturbances or erosion prevention measures (Fig. 8). Also, buildings and other structures can be added to create anthropogenic environments and simulate interactions between natural processes and human activities. The scale models are based on real-world data, in our case 1–2 m land surface topographic contours derived from bare Earth, LiDAR-based DEMs. The accuracy of the initial model can be adjusted to the desired level using the projected differences between the original and the georeferenced scanned model elevations. The system set-up is very open and allows users to bring their own 3D scale models, geospatial data and laptops with any software capable of generating images from the scanned point cloud analyses.

To provide background information for the modification, various GIS data layers (e.g., orthophotography, planimetry, contours, streams, flow accumulation) can be projected over the 3D model. The model is then modified and scanned at any time when feedback on the modification impact is needed. After each scan, the point cloud is imported into GIS and a new DEM is computed along with the user selected parameters of interest, such as slope, aspect, contours, flow accumulation, and any other parameter available in the GIS relevant to the studied problem. The results of the analysis are projected over the model to provide rapid feedback on impacts of introduced terrain changes on topographic parameters and flow patterns. Dynamic hydrologic, erosion or solar irradiation simulations can also be performed for the modified landscapes and the results can be projected over the scale model as animations (Fig. 8 and the linked video). In this way, various aspects of landscape dynamics and impacts of terrain change on processes can be studied. TanGeoMS has also proved useful for geospatial software development work as it allowed us to quickly generate large number of different terrain configurations with rapid feedback for the testing of flow routing algorithms (Fig. 8) and robust point cloud processing tools.

4. Case studies

Application of the presented visualization techniques as supporting tools for analyses of landforms and landscape evolution in regions with contrasting geomorphology mapped by airborne LiDAR is illustrated by two case studies from North Carolina, USA (Fig. 9). Mountain geomorphology was studied in an area within the Great Smoky Mountains National Park that includes numerous debris flows and was mapped recently by multiple return airborne LiDAR. Dynamic coastal landforms on a barrier island along the Outer Banks, North

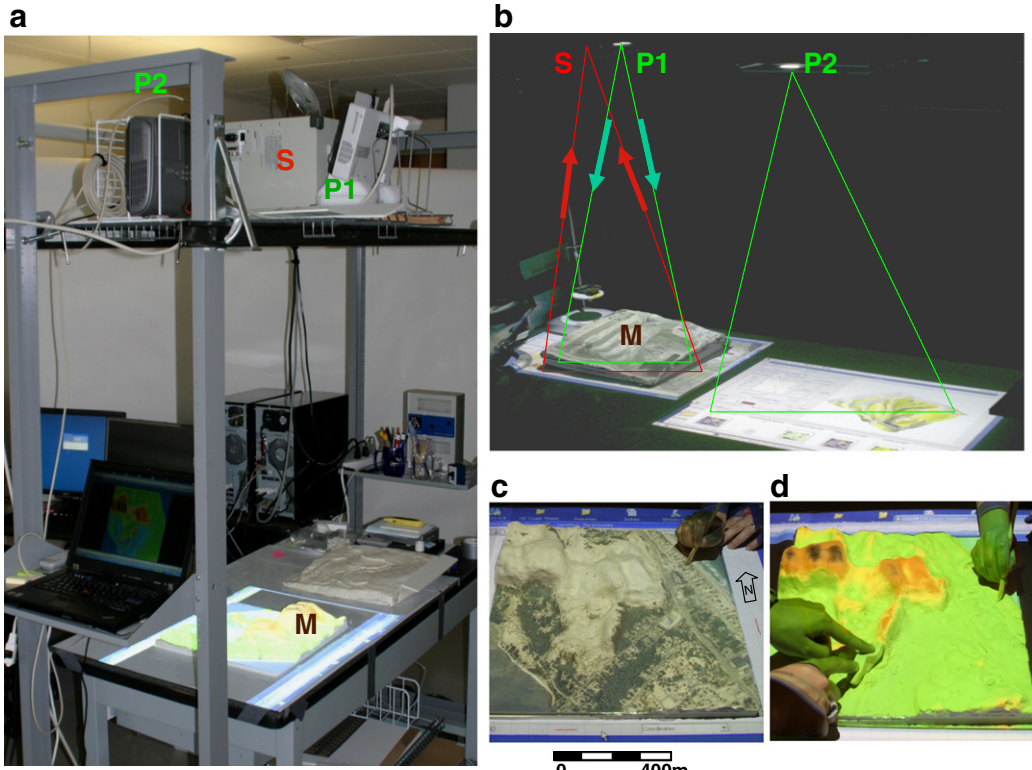


Fig. 7. TanGeoMS: (a) the configuration includes a flexible scale model **M**, 3D laser scanner **S**, two projectors **P**₁ and **P**₂ coupled with workstations or laptops and GRASS GIS; (b) projector **P**₁ is aligned with the scanner **S** so that the results of the scanned model analysis can be readily projected back over the model, additional results can be projected over the flat tabletop along with the GIS user interface to support data query or interactive 3D perspective views; (c) projected orthophotography provides background information to guide terrain modifications; (d) more than one user can modify the model and collaborate on the design.

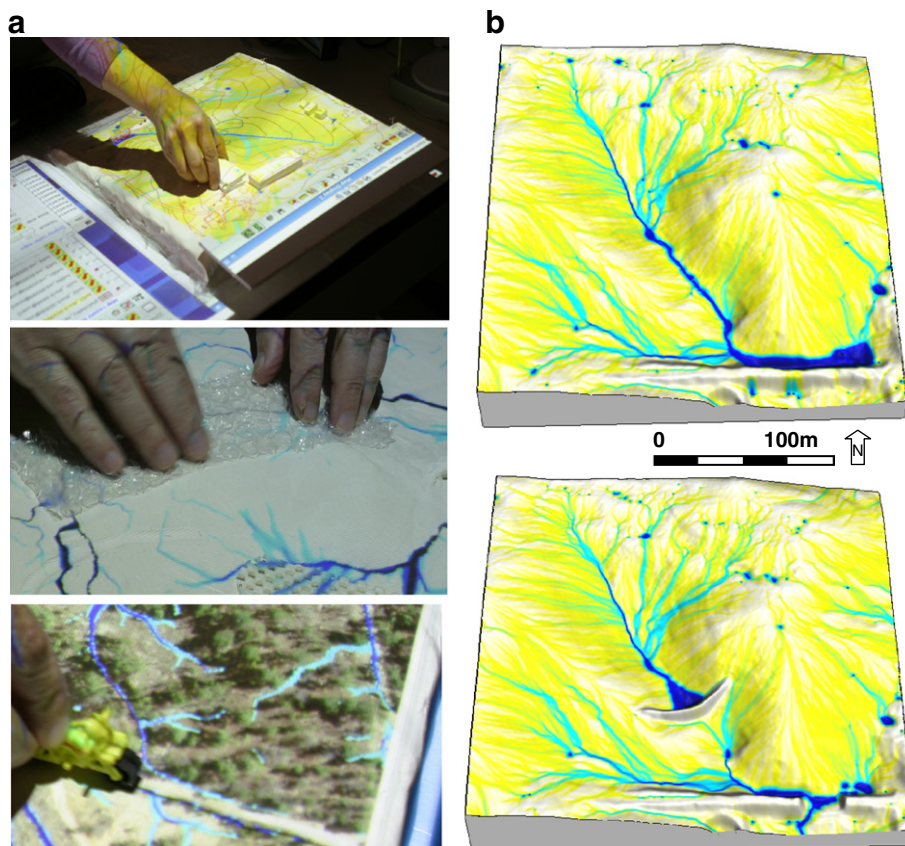


Fig. 8. Testing robustness of flow routing algorithms by modifying an initial bare Earth 3D model: (a) adding buildings, rip-rap and a dirt road tracks; (b) water flow pattern on the initial and modified elevation model simulated by a path sampling approach that can handle structures and rough surfaces with depressions; (see also video of dynamic experiments at http://skagit.meas.ncsu.edu/~helena/wrriwork/tangis/tg1bak2_ed4_1min640.mov).

Carolina were analyzed and visualized based on time series of elevation data. TanGeoMS was used to explore impact of storm surge for different scenarios of landform evolution and sea level elevation.

4.1. Mountain geomorphology

The first case study provides an example of static, multiple surface visualization as a tool to support identification and characterization of

recent debris flows on the steep slopes of the southern Appalachian Mountains. This study has started recently and, at this stage, visualization has been used to guide the direction of geospatial analysis and field research planning.

The location and characteristics of the shallow landslides have been traditionally mapped using aerial imagery and selected field traverses (Southworth et al., 2005). Recent multiple return LiDAR mapping of western North Carolina provides the opportunity to identify previously unmapped or recent debris flows and derive additional information

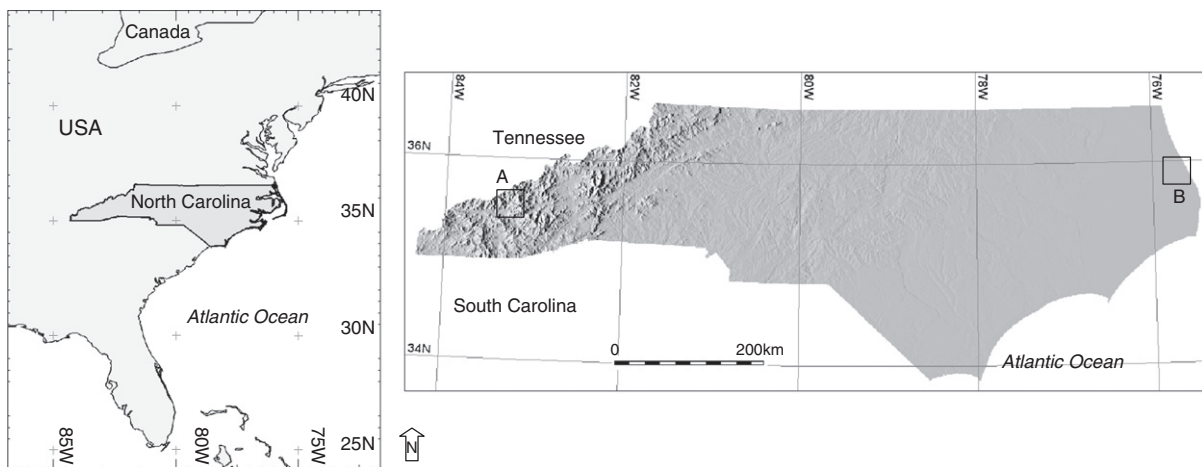


Fig. 9. Location of case studies regions A (in the Great Smoky Mountains National Park) and B (on the Outer Banks barrier islands) in North Carolina, USA.

about the structure and properties of the ones previously identified. Visualization techniques have been essential for the assessment of information that can be derived from the LiDAR-based surfaces and to guide the analysis of spatial relationship between geology, vegetation and landslide locations.

A color map representing geology draped over the bare Earth DEM displayed in 3D perspective provided insight into the relation between geology (Southworth et al., 2005) and landforms geometry in the Bradley Fork watershed (Fig. 10). The highly resistant slate of the Anakeesta Formation inhibits erosion, explaining the steep, sharp slopes in the upper section of this watershed. Deposits of alluvium and debris fans form wide, low slope areas.

To visually evaluate several approaches to recent debris flows identification and characterization the elevation surface with vegetation was interpolated from the multiple return LiDAR point cloud at 3 m resolution and displayed in 3D perspective with two light sources. The illumination highlights the difference between the rough surface of forested areas and smoother, bare or sparsely vegetated debris flows (Fig. 11a). Several surface geometry parameters were computed and displayed as color maps over an illuminated relief to visually assess the relation of these parameters to potential debris flows scars (see the slope map in Fig. 11b). Preliminary extraction of the debris flows has been performed by combining threshold values for slope, profile curvature and flow path length using map algebra, with the result again displayed as color map on 3D perspective view. Flow accumulation pattern was then derived for these areas using D-infinity approach (Neteler and Mitasova, 2008, Section 5.4.4) and displayed as masked raster over illuminated topography. This visualization highlights the differences between the narrow debris flows with single channels and the broad bare areas with multiple parallel channels (Fig. 11d).

Visual analysis of the 3D views served as a preliminary assessment of the methods' capability to map recent debris flows, and as a guide to more detailed spatial statistical analysis of the relationship between the parameters that can be derived from multiple return

LiDAR data and debris flows – with the goal to develop methodology for rapid automated mapping of debris flows. An on-going field study is being performed to evaluate the accuracy of the LiDAR-based methods and compare them with the 2D image based methods.

Within the neighboring Frowning Rock Prong watershed, relief shading was successfully used to identify artifacts in high resolution LiDAR-based DEM (Fig. 12). It revealed an apparent shift in elevation data along the LiDAR swath edges when applied to a 2 m resolution DEM interpolated from the multiple return points, an artifact which is hard to identify on a contour or 2D color map. Relief shading of the interpolated bare Earth surface indicates that the artifact has been removed from the bare Earth point data.

To visually explore relationship between the morphology of bare Earth surface and vegetation height the bare Earth and first return DEMs were displayed together and a vertical cutting plane was interactively moved and rotated across the watershed. When passing through the areas with known debris flows, the mature, high forest cover, typical for this area, transitioned into bare Earth or very low vegetation (Fig. 13). Field surveys are being performed to relate the height of vegetation extracted from the multiple return data to the age of the debris flows, with visualization providing valuable information for field research planning.

4.2. Barrier island dynamics

The second case study on dynamics of barrier island dunes represents multiyear research that utilizes a dense set of elevation data time series. Throughout this project, visualization has been used extensively to assist with data processing, to gain insight into spatial patterns of sand transport and to investigate impacts of storm surge for different dune management scenarios. The techniques for data processing and for feature-based geospatial analysis were presented by Mitasova et al. (2005a, 2005b), here we focus on the role of visualization in this project and extend our previous work by adding

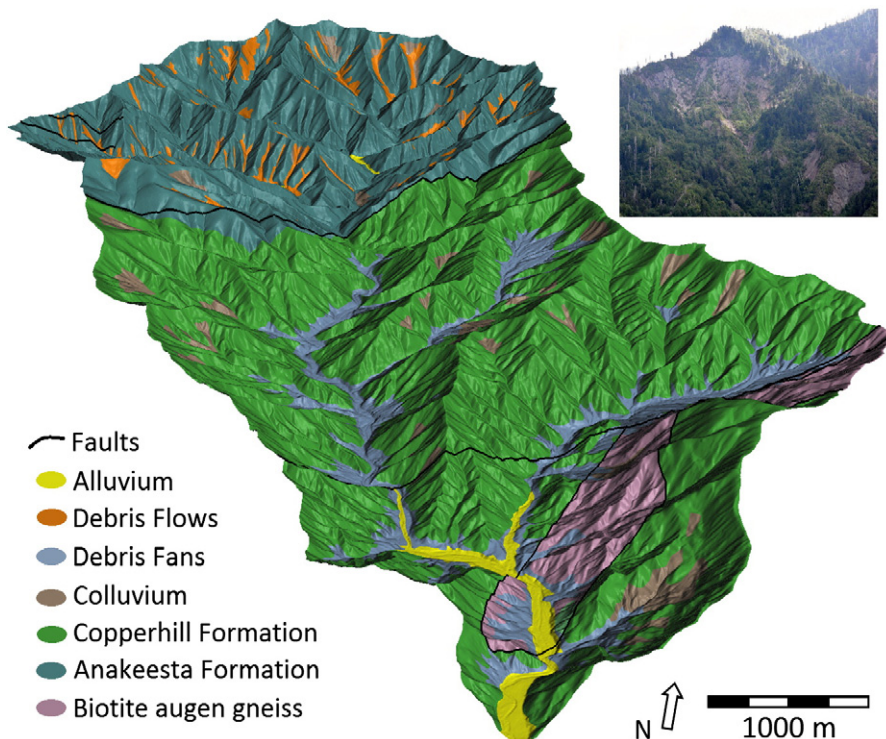


Fig. 10. Geology map draped over DEM highlights the relationship between the elevation surface geometry and bedrock and surficial geology of the Bradley Fork watershed (data from Southworth et al., 2005).

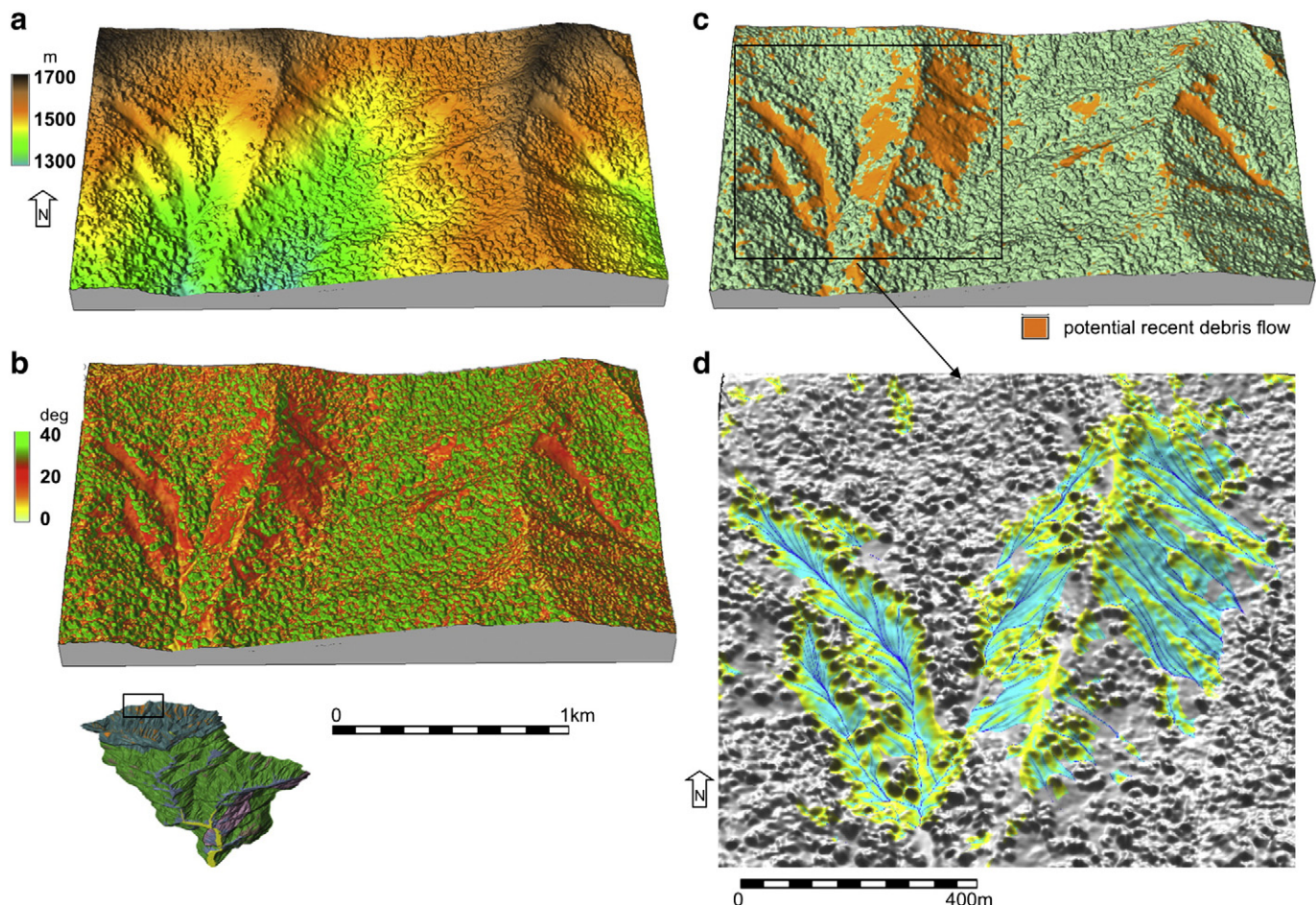


Fig. 11. Multiple return elevation surface representing a headwater area within the Bradley Fork watershed displayed at 3 m resolution with color maps representing derived parameters relevant for identification of debris flows: (a) elevation color map draped over 3D perspective view of topography with vegetation; (b) slope map with lower, continuous values in the debris flow areas and very high, scattered values in the forested areas reflecting presence of large trees; (c) color map representing potential debris flows scars derived from combination of slope, curvature and flowpath length parameters; (d) flow accumulation pattern within debris flows.

the raster and voxel based analysis and new results based on the LiDAR data that were acquired in the years 2007 and 2008.

The study area, located within the 162-hectare Jockey's Ridge State Park, includes the largest active dune system on the Atlantic coast of North America (Fig. 14). Over the past 50 years, the main dune has lost almost half of its elevation (Fig. 15) and the smaller dunes keep migrating outside the park boundaries. The park management has been transporting the sand that left the park to the windward side of the main dune in an effort to stop the loss of elevation. To better understand the ongoing dune transformation, quantify the changes, and assess the effectiveness of the current dune management, evolution of the dune system was investigated using time series of 1 m resolution DEMs interpolated from photogrammetric and LiDAR data for years 1974, 1995, 1998, 1999, 2001, 2007 and 2008.

As in the previous case study, surface visualization with interactive lighting was an effective tool for identification of subtle natural or anthropogenic features as well as artifacts in the data (Fig. 14) and guided the processing of the DEMs. Positioning the light source far enough from the zenith (in our case, 40° above horizon), and in northwest direction revealed a “corduroy effect” on the interpolated dune surface that follows the LiDAR point sampling pattern. To remove the effect, the data were re-interpolated with adjusted parameters. Low positioned light source also uncovered the structure of stabilization fences and subtle features in flat areas, created by

sand accumulated around vegetation (Fig. 14b). To capture the directional features, such as the LiDAR scanning pattern and the fences, the light source azimuth was interactively set orthogonal to the direction of the features (Smith and Wise, 2007). Positioning the light source close to the zenith diminishes the visibility of subtle terrain features regardless of its azimuth (Fig. 14b).

Evolution of the dunes was visualized by surface overlays in 3D perspective view, combined with transparency (Fig. 15), and using cross-sections derived by interactive cutting planes across two overlaid DEMs for the years 1974 and 2008 (Fig. 16). They confirm the loss of sand on the windward side of the dune and significant gain in elevation on the leeward side (Fig. 16). Several sets of animations, using different viewing positions and draped color maps, revealed the complex dynamics of the dune system migration that combines the general southward translation with clockwise rotation. An animation with low viewing position from the sound was used to communicate the loss of elevation that accompanied the southward migration of the dune system. An animation from overhead view with draped slip faces extracted from the slope maps provided insights into the transformation of the dunes from the crescentic form to sand-starved parabolic type, starting with the lower east dune (1974–1998) and followed most recently by the main dune (Fig. 17). Display of the change in the locations of dune peaks over time as point symbols in 3D perspective over the 2008 year DEM (Fig. 16) further highlights the

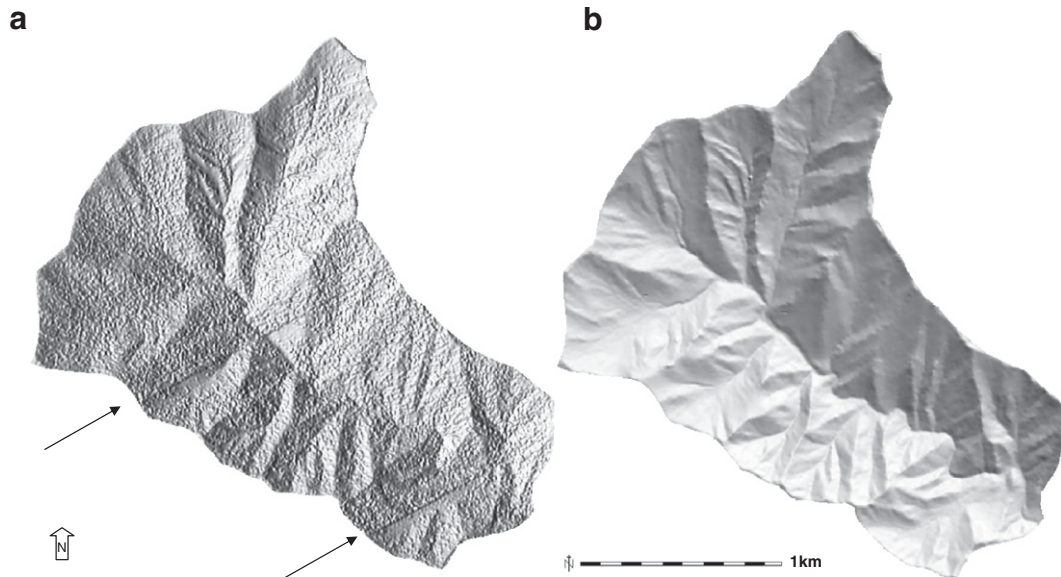


Fig. 12. Analysis of the Frowning Rock Prong watershed in the Great Smoky Mountains National Park: (a) multiple return shaded relief map: two swath edge elevation shifts are clearly visible, (b) bare Earth relief shading map does not show any significant artifacts.

dramatic loss of elevation for the main dune and gradual stabilizing of the entire dune system at the elevation level of 20–22 m observed at the beginning of the 20th century.

A more detailed analysis of landform dynamics was performed for the Jockey's Ridge east dune and the neighboring beach-foredune system using 0.5 m resolution DEMs derived from LiDAR data

acquired in 1997, 1998, 1999, 2001, 2004, 2005, 2007, and 2008. The core and envelope surfaces provided insight into spatial and temporal patterns of terrain dynamics and were visually analyzed using interactive cutting planes (Fig. 18). Large differences between the core and envelope indicate locations with significant changes in elevations that were also captured in a color map of elevation range

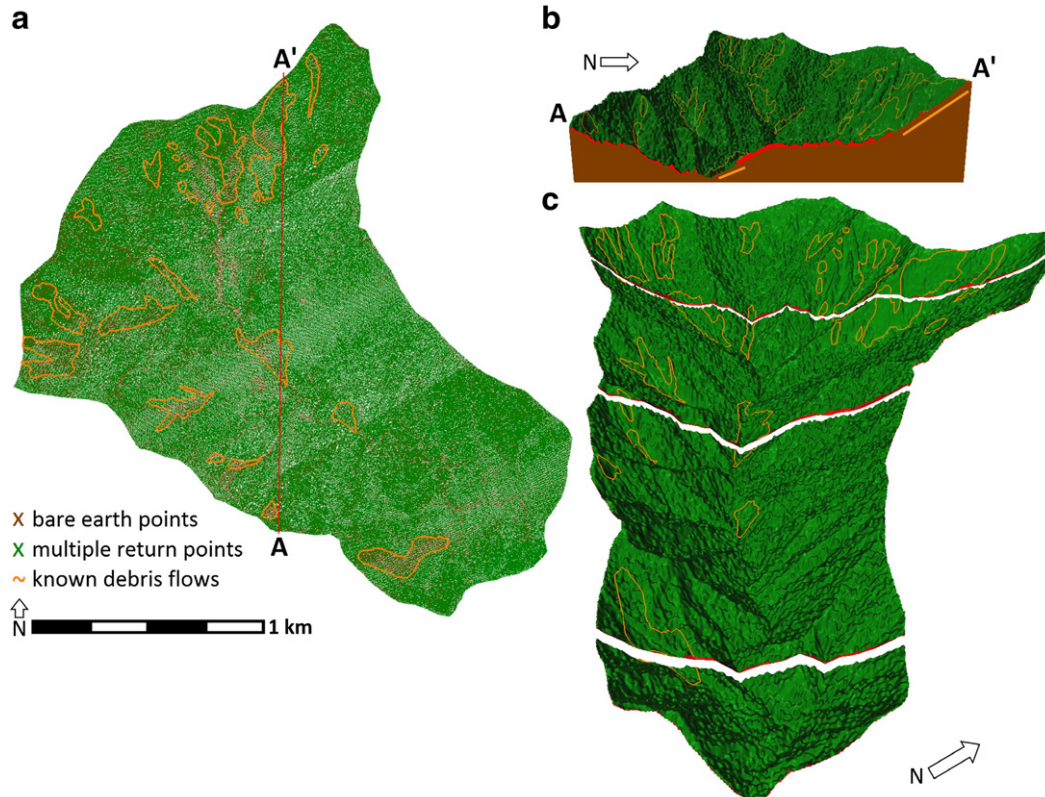


Fig. 13. Multiple return and bare Earth elevation data in the Frowning Rock Prong watershed: (a) sparse bare Earth and dense, almost continuous multiple return LiDAR points overlain with known locations of debris flows published by Southworth et al. (2005); (b) detailed view of a A–A' cross-section, red layer shows vegetation height as difference between the multiple return and bare Earth elevations with almost no vegetation in the debris flow area; (c) cutting planes across overlain bare Earth and multiple return surfaces.

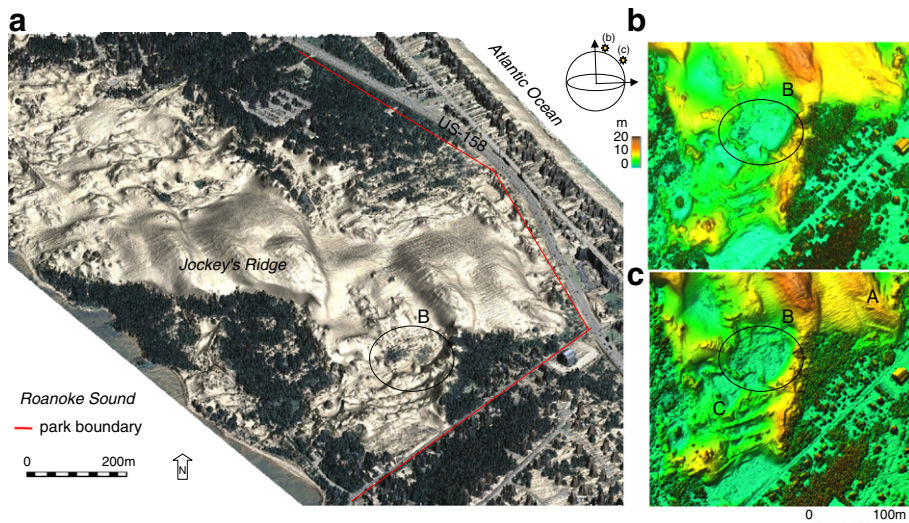


Fig. 14. Jockey's Ridge dune system: (a) orthophoto draped over the 3D perspective view of the 1 m resolution, year 2008 DEM, (b) 3D perspective view illuminated from the light source close to the zenith (c) illumination by the light source farther from the zenith coming from northwest direction reveals the corduroy artifact on dunes (A), subtle features in flat areas (B) and structure of fences (C). The surface elevation is exaggerated 3-times.

draped over the most recent DEM. The migrating east dune has experienced the largest range of naturally driven elevation change and the new or lost buildings had the highest change among structures. Time of maximum raster map highlights the southward migration of the maximum elevations on the dune (Fig. 18a). Evolution of the actual elevation surfaces within the dynamic layer was visualized using animations within a selected cross-section (Fig. 18c).

Trivariate interpolation of elevation in space-time domain was used to create a voxel model of the east dune dynamics and to visualize evolution of selected contours as isosurfaces (Fig. 19). Topology of these isosurfaces was studied in relation to the processes that control the dynamics of topography in these locations. Stable elevation levels (no change in the contour location and shape over time) are represented by isosurfaces that are vertical extrusions of the initial contour at time t_1 . A

typical example in our case study was a 6 m contour extracted from a stable building (Fig. 19). None of the isosurfaces extracted at the east dune location at the 6 m elevation and above was vertical, indicating that the entire volume of sand above 6 m moved. The isosurfaces show that the movement was complex with migration over the entire spectrum of directions from east to south and with higher migration rates at higher elevations than at the lower levels (Fig. 19).

Exploratory TanGeoMS analysis was used to investigate the impact of different approaches to dune management and impact of foredune breaches on the spatial pattern of storm surge flooding. First, a 1:3000 scale model was built using contours derived from the 2007 bare Earth DEM. The model was covered by plasticine, scanned, georeferenced and compared with the original data. At this scale, the level of detail that we were able to work with was comparable to 4–6 m

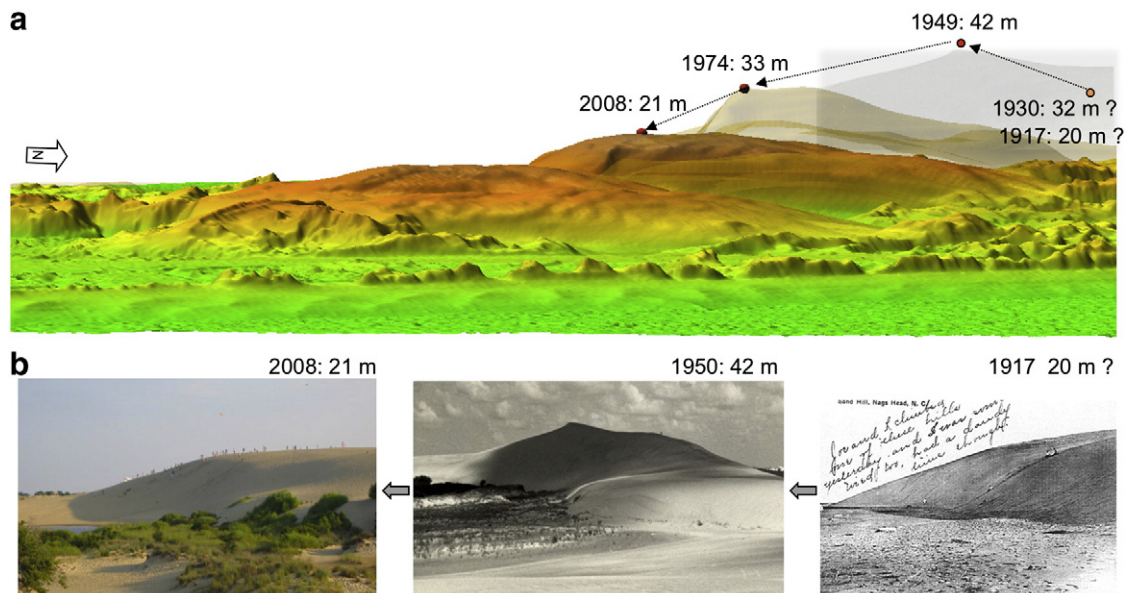


Fig. 15. Evolution of the Jockey's Ridge sand dune: (a) 3D perspective view of the dunes from the ocean using overlaid DEMs for the years 2008 and 1974 (semitransparent), and an inserted transparent photo for the year 1949 placed at the known location of the 1949 peak (neither contours nor DEM are available for 1949); (b) the current and historical photos indicate that the dune has grown rapidly between 1917 and 1950 and has been returning to its early 20th century form.

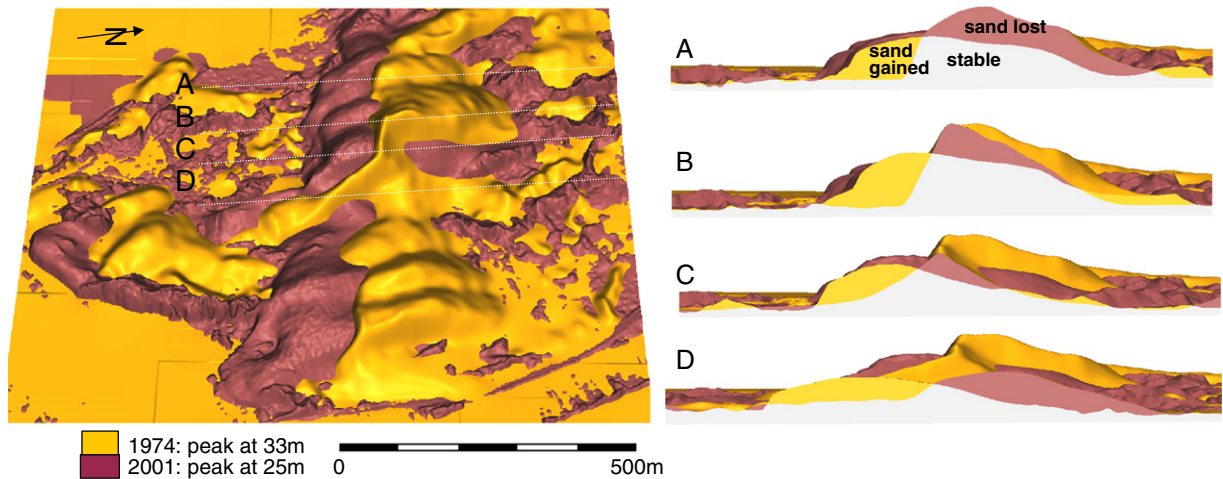


Fig. 16. Elevation surfaces overlay and cross-sections: Jockey Ridge sand dune 1974–2008 add the peak image.

resolution DEMs (compared to the typical 1 m resolution detail used in the small watershed studies at 1:1200 scale, Tateosian et al., 2010). This was sufficient, however, for investigations of sand relocation and dune breach impacts on storm surge flooding that are typically done at 10–50 m resolution.

The surface of the initial model was modified by hand to create new landscape configurations, scanned, the flooding simulations were performed for the new DEMs and the results projected over the model as images or animations. Preliminary results from these experiments are illustrated in Fig. 20. The simulations performed for the year 2007

DEM show that the area starts flooding from the soundside at a relatively low levels of storm surge at 1.5 m, whereas the ocean side can withstand surge levels as high as 4 m, assuming that the protective foredunes will not be breached. To investigate potential extent of flooding that would be caused by a single or multiple breaches in these dunes at different locations, we have breached the foredunes by carving out the clay with a craft tool (Fig. 20) and repaired the dunes simply by putting back a piece of clay. The modified model was scanned, the flooding was recomputed and the results were projected over the model to provide feedback for further

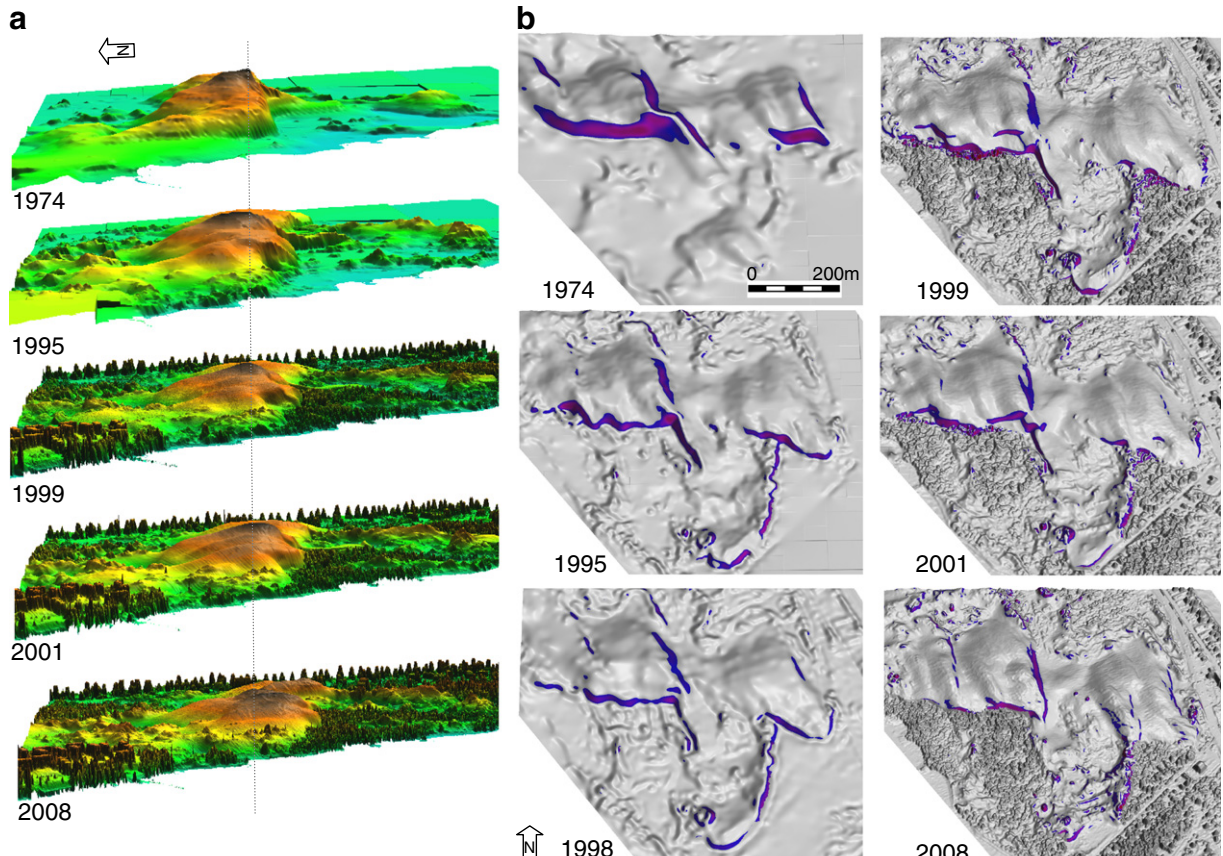


Fig. 17. Frame sequences used for animations: (a) lower, west side view shows horizontal migration with gradual loss of elevation, (b) animation with draped slip faces reveals transformation from crescentic to parabolic dunes.

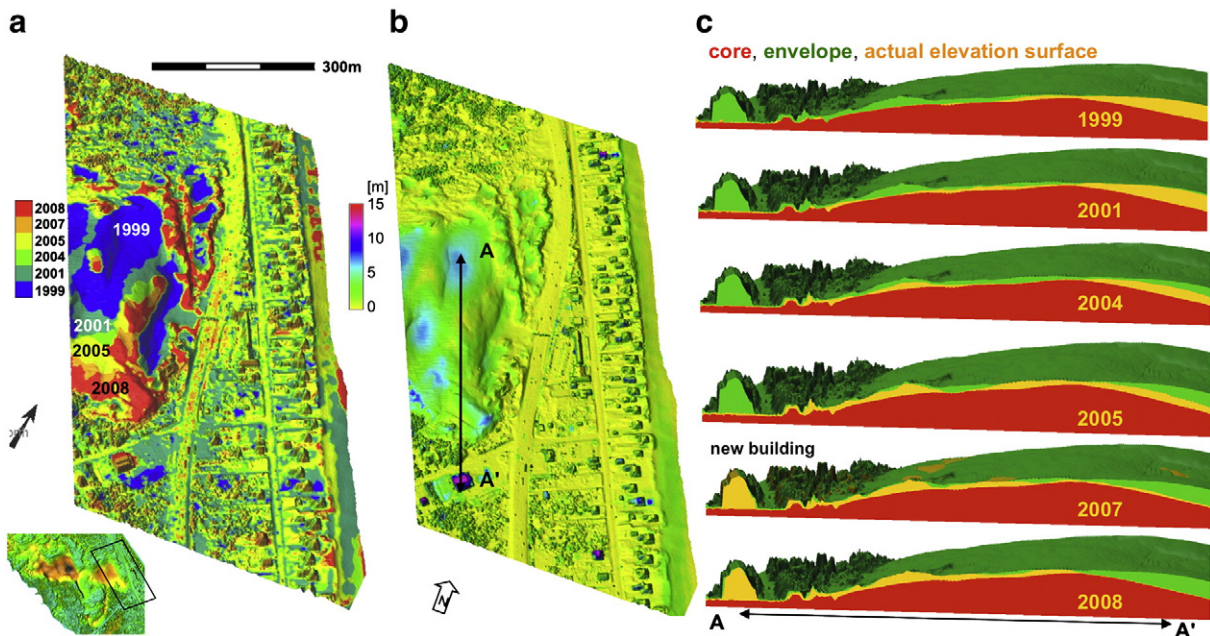


Fig. 18. New type of maps representing terrain dynamics based on time series of DEMs derived from LiDAR data: (a) time of maximum map represents the year when each grid cell was at the maximum elevation; (b) elevation range map; (c) frames from animation visualize evolution of actual elevation surface within the dynamic layer defined by the core and envelope surfaces.

exploration. The projected results demonstrate that even a small breach can cause extensive flooding because of low elevation in the back island areas.

We have also investigated the possibilities to reduce the flooding from the sound side. For example, we have added back the small south dune that was removed from the park in the year 2003 because its migration was threatening the neighboring homes and road (Mitasova et al., 2005a). Also, we have extended its edge in the direction of its migration closer to the sound (Fig. 20), scanned the modified model, rerun the simulation and projected the results over the model.

Although this change would require relocation of the small access road, the extended dune would provide protection from the flooding that is quite common here which affects a large area.

5. Conclusions

Modern mapping techniques that produce massive, highly detailed elevation data have increased the role of scientific visualization in analysis and communication of information about land surface, its properties, features and evolution. In addition to standard

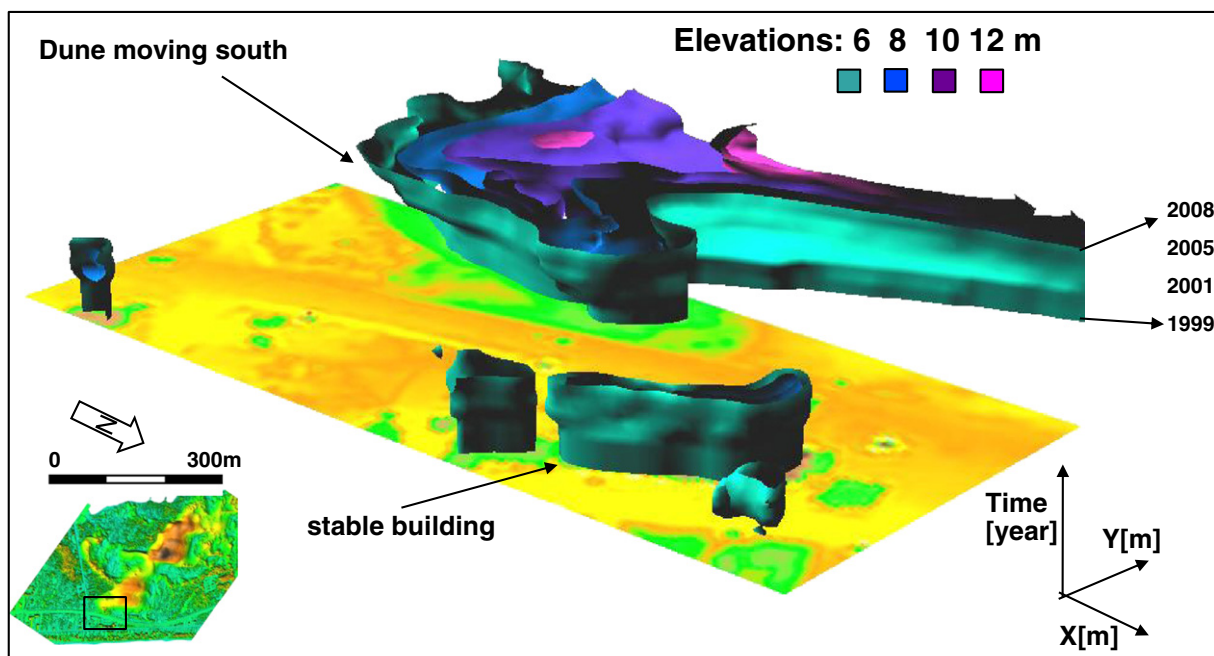


Fig. 19. Evolution of elevation contours for a section of the east dune visualized as isosurfaces extracted from voxel representation of terrain dynamics; 6, 8, 10 and 12 m elevation contour change during years 1999 to 2008.

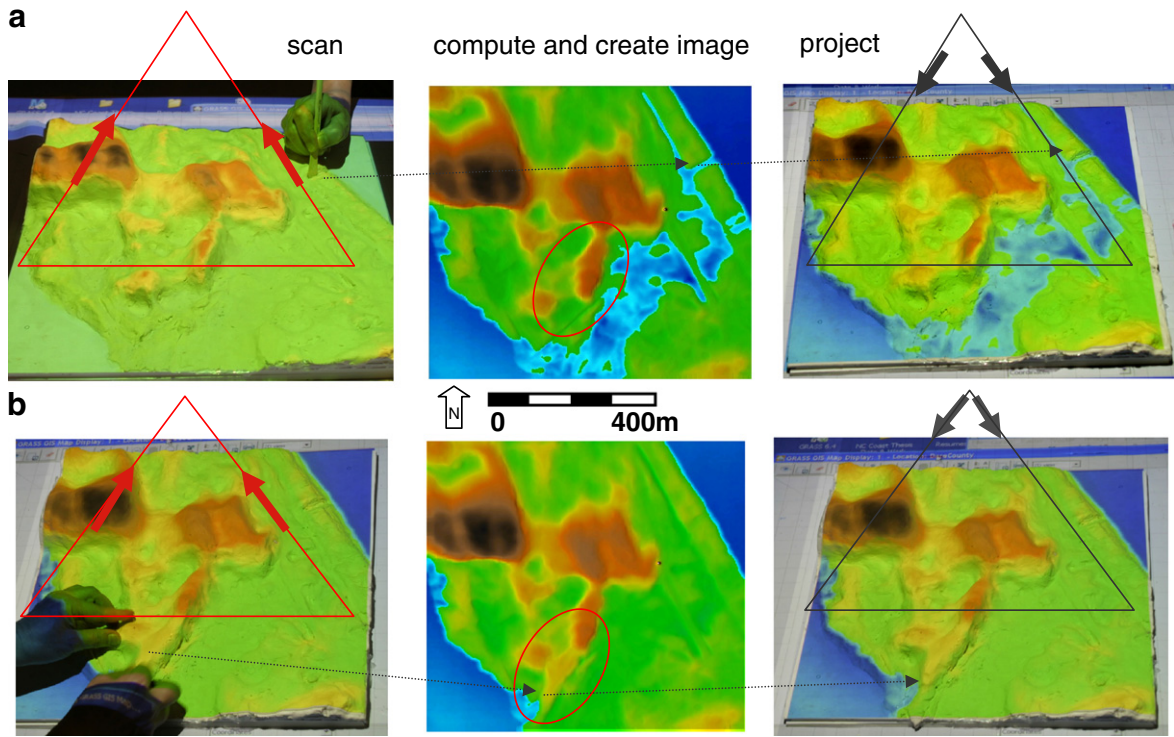


Fig. 20. Exploring the impact of different landscape configurations on coastal flooding using TanGeoMS: (a) flood simulations with foredune breach, (b) flood simulation with the added sand dune and filled breach.

relief shading, 3D perspective views of interactively illuminated surfaces using multiple light sources have become the core techniques for visualization of high resolution terrain models. Multiple return LiDAR data and efficiency of repeated topographic surveys expanded the use of 3D interactive visualization to multiple surfaces as demonstrated by the presented applications to debris flow analysis in mountainous region and investigations of costal terrain dynamics. New concepts of *n*-year core and envelope surfaces were introduced to measure complex spatial patterns of terrain evolution from time series of LiDAR data along with 3D animations.

The space-time voxel model of terrain evolution is a technique at early stages of development, but it holds the most promise for elevation time series analysis with a large number of time snapshots where contour overlays or side-by-side views of DEMs are not practical. Additional research is needed to develop interpretations of space-time isosurface topology and its relation to geomorphological processes.

The Tangible Geospatial Modeling System expands the increasingly common touch technology and multi-modal computer interfaces to 3D space to support more intuitive and collaborative interaction with topographic data. The case study demonstrated that numerous modifications can be created and explored quickly in a collaborative environment so that only the most promising solutions then need to be transformed into more accurate designs, based on real-world data and computer aided design tools, using the modified 3D scan as a sketch. Although the affordable 3D scanners needed for widespread use of this type of systems are not yet available, the presented examples illustrate the potential of tangible interaction with terrain models with rapid feedback on impacts of modifications on terrain parameters and processes. In addition to its original purpose as a tangible interface TanGeoMS has proved invaluable for development work and as a teaching tool. Recently introduced handheld laser scanners with fast 3D model registration, mini-projectors and increasingly common 3D printers and computer guided carving

tools create further potential for the expansion of the tangible geospatial modeling concept, including potential mobile systems.

Finally, scientific visualization of geospatial data is a broad field and our focus was on a subset of techniques that are highly relevant for geomorphology and take advantage of the high resolution LiDAR data time series that have become available only recently. We have highlighted the visualization capabilities of a freely available, open source geospatial software (in our case GRASS GIS module nviz) that provides opportunities for researchers and developers to adjust or improve the code according to their needs and contribute back to the community. The most active development in the open source geospatial community combines the web mapping techniques with sophisticated analysis and we anticipate that the upcoming increase in speed of wireless Internet connections, Web GIS services will make the complex scientific visualization of landscapes based on high resolution elevation data readily available in laboratory and mobile environments.

Acknowledgements

The authors would like to gratefully acknowledge the funding support from the US Army Research Office and North Carolina Sea Grant as well as the free access to the LiDAR data provided by the United States Geological Survey, US Army Corps of Engineers, North Carolina Floodplain Mapping Program and the National Oceanic and Atmospheric Administration Coastal Services Center.

References

- Andrews, B.D., Gares, P.A., Colby, J.D., 2002. Techniques for GIS modeling of coastal dunes. *Geomorphology* 48 (1–3), 289–308.
- Baru, C., Keller, R., Wallet, B., Crosby, C., Moreland, J., Nadeau, D., 2008. Integrating diverse geophysical and geological data to construct multi-dimensional earth models: the open earth framework. AGU Fall meeting (Abstracts, #IN51A-1147).

- Bellian, J.A., Kerans, C., Jennette, D.C., 2005. Digital outcrop models: applications of terrestrial scanning LiDAR technology in stratigraphic modeling. *Journal of Sedimentary Research* 75, 166–176.
- Billen, M.I., Kreylos, O., Hamann, B., Jadamec, M.A., Kellogg, L.H., Staadt, O., Sumner, D.Y., 2008. A geoscience perspective on immersive 3D gridded data visualization. *Computers and Geosciences* 34, 1056–1072.
- Boschetti, L., Roy, D.P., Justice, C.O., 2008. Using NASA's World Wind virtual globe for interactive Internet visualization of the global MODIS burned area product. *International Journal of Remote Sensing* 29 (11), 3067–3072.
- Buckley, A., Hurni, L., Kriz, K., Patterson, T., Olsenholter, J., 2004. Cartography and visualization in mountain geomorphology. In: Bishop, M.P., Shroder, J.F. (Eds.), *Geographic Information Science and Mountain Geomorphology*. Springer-Praxis, NY, pp. 253–287.
- Coucelo, C., Duarte, P., Crespo, R., 2005. Combining 3D solid maps with GIS data video projection. Paper No. 434. Proc. 2nd International Conference on Geographic Information GIS Planet, Estoril, Portugal (CDROM).
- Dangermond, Jack, 2009. GIS: designing our future. ArcNews. (summer) <http://www.esri.com/news/arcnews/summer09articles/gis-designing-our-future.html> (accessed 6 July, 2010).
- Defanti, T.A., Dawe, G., Sandin, D.J., Schulze, J.P., Otto, P., Girado, J., Kuester, F., Smarr, L., Rao, R., 2009. The StarCAVE, a third-generation CAVE and virtual reality OptIPortal. *Future Generation Computer Systems* 25 (2), 169–178.
- Defense Update, 2005. The Modern Command Post Tactical Operations Center, Defense Update, International Online Defense Magazine 3, 8. <http://defense-update.com/features/du-3-05/c4i-8.htm> (2005) (accessed 7 June 2010).
- Directions Staff, 2004. 'WOW Technology' found among the many exhibitors at the ESRI user's conference, directions magazine. http://www.directionsmag.com/article.php?article_id=6412004 (accessed 7 June 2010).
- Earth Remote Sensing Data Analysis Center, 2009. ASTER Global Digital Elevation Model. <http://www.gdem.aster.ersdac.or.jp/> (2009) (accessed 10 July, 2010).
- Gesch, D., Evans, G., Mauck, J., Hutchinson, J., Carswell Jr., W.J., 2009. The National Map—Elevation: U.S. Geological Survey Fact Sheet 2009–3053 (4 pp.).
- Heritage, G., Hetherington, D., 2007. Towards a protocol for laser scanning in fluvial geomorphology. *Earth Surface Processes and Landforms* 32 (1), 66–74.
- Horn, B.K.P., 1981. Hill shading and the reflectance map. *Proceedings of the Institute of Electrical and Electronics Engineers (IEEE)* 69 (1), 14–47.
- Johnson, A., Leigh, J., Morin, P., Van Keeken, P., 2006. GeoWall: stereoscopic visualization for geoscience research and education. *IEEE Computer Graphics and Applications* 26 (6), 10–14.
- Johnston, D.M., 1998. TRACES: revealing nature through models of landscape dynamics. *Landscape Journal* 17, 4–5.
- Kraak, M.J., Madzudzo, P.F., 2007. Space time visualization for epidemiological research. *Proceedings of the 23rd International Cartographic Conference ICC: Cartography for Everyone and for You*, 4–10 August 2007 Moscow, Russia. International Cartographic Association (ICA), Moscow, Russia (13 pp.).
- Krum, D.M., Omoteso, O., Ribarsky, W., Starner, T., Hodges, L.F., 2002. Evaluation of a multimodal interface for 3D terrain visualization. *Proceedings of the conference on Visualization'02*, pp. 411–418.
- Lin, C.R., Lofton, R.B., 1998. Application of virtual reality in the interpretation of geoscience data. *Proceedings ACM Special Interest Group on Computer Graphics and Interactive Techniques Symposium on Virtual Reality Software and Technology*, Taipei Taiwan, pp. 187–194.
- Lowe, J.W., 2004. Revealing in raster data, Geospatial Solutions, October 2004, pp. 46–49. <http://www.giswebsite.com/pubs/200410/nr200410.pdf> (accessed 5 June, 2010).
- Luo, W., Duffin, K.L., Peronja, E., Stravers, J.A., Henry, G.M., 2004. A Web-based Interactive Landform Simulation Model (WILSIM). *Computers and Geosciences* 30 (3), 215–220.
- Marshal, P., 2004. XenoVision gives new meaning to visualizing the battlefield, Federal Computer Week, Sep. 13, 2004. <http://fcw.com/articles/2004/09/13/xenovision-gives-new-meaning-to-visualizing-the-battlefield.aspx> (accessed 7 June 2010).
- Mitas, L., Brown, W.M., Mitasova, H., 1997. Role of dynamic cartography in simulations of landscape processes based on multi-variate fields. *Computers and Geosciences* 23 (4), 437–446.
- Mitasova, H., Mitas, L., Brown, W.M., Gerdes, D.P., Kosinovsky, I., 1995. Modeling spatially and temporally distributed phenomena: new methods and tools for GRASS GIS. *International Journal of Geographic Information Systems* 9 (4), 433–446.
- Mitasova, H., Overton, M., Harmon, R.S., 2005a. Geospatial analysis of a coastal sand dune field evolution: Jockey's Ridge, North Carolina. *Geomorphology* 72, 204–221.
- Mitasova, H., Mitas, L., Harmon, R.S., 2005b. Simultaneous spline interpolation and topographic analysis for LiDAR elevation data: methods for Open source GIS. *IEEE Geoscience and Remote Sensing Letters* 2 (4), 375–379.
- Mitasova, H., Mitas, L., Ratti, C., Ishii, H., Alonso, J., Harmon, R.S., 2006. Real-time human interaction with landscape models using a tangible geospatial modeling environment. *IEEE Computer Graphics & Applications, Special Issue—GeoVisualization* 26 (4), 55–63.
- Mitasova, H., Overton, M., Recalde, J.J., Bernstein, D., Freeman, C., 2009. Raster-based analysis of coastal terrain dynamics from multitemporal lidar data. *Journal of Coastal Research* 25 (2), 507–514.
- Napieralski, J., Harbor, J., Li, Y., 2007. Glacial geomorphology and geographic information systems. *Earth-Science Reviews* 85 (1–2), 1–22.
- Neteler, M., Mitasova, H., 2008. Open Source GIS: A GRASS GIS Approach, Third edition. Springer, NY, p. 406.
- NOAA Coastal Services Center, 2010. Digital Coast. <http://www.csc.noaa.gov/digitalcoast/data/> (accessed 10 July, 2010).
- Prentice, C.S., Crosby, C.J., Whitehill, C.S., Arrowsmith, J.R., Furlong, K.P., Phillips, D.A., 2009. Illuminating Northern California's Active Faults. *Eos* 90 (7), 55–56.
- Rabus, B., Eineder, M., Roth, A., Bamler, R., 2003. The shuttle radar topography mission – a new class of digital elevation models acquired by spaceborne radar. *Journal of Photogrammetry and Remote Sensing* 57, 241–262.
- Ratti, C., Wang, Y., Ishii, H., Piper, B., Frenchman, D., 2004. Tangible User Interfaces (TUIs): a novel paradigm for GIS. *Transactions in GIS* 8 (4), 407–421.
- Schöning, J., Steinicke, F., Kruger, A., Hinrichs, K.H., 2009. Interscopic multi-touch surfaces: using binocular interaction for intuitive manipulation of spatial data. *Proceedings of IEEE Symposium on 3D User Interfaces*. IEEE Press, pp. 127–128.
- Sithole, G., Vosselman, G., 2004. Experimental comparison of filter algorithms for bare-Earth extraction from airborne laser scanning point clouds. *ISPRS Journal of Photogrammetry and Remote Sensing* 59, 85–101.
- Smith, M.J., Clark, C.D., 2005. Methods for the visualization of digital elevation models for landform mapping. *Earth Surface Processes and Landforms* 30 (7), 885–900.
- Smith, M.J., Wise, S.M., 2007. Problems of bias in mapping linear landforms from satellite imagery. *International Journal of Applied Earth Observation and Geoinformation* 9, 65–78.
- Sorokine, A., 2007. Implementation of a parallel high-performance visualization technique in GRASS GIS. *Computers and Geosciences* 33 (5), 685–695.
- Southworth, S., Schultz, A., Deneney, D., 2005. Geologic map of the Great Smoky Mountains National Park Region, Tennessee and North Carolina: U.S. Geological Survey Professional Report 2005–1225 and Geological Map (1:100,000 scale), pp 116.
- Tanimoto, S.L., Pavlidis, T., 1975. A hierarchical data structure for picture processing. *Computer Graphics and Image Processing* 4 (2), 104–119.
- Tateosian, L.G., Mitasova, H., Harmon, B., Fogelman, B., Weaver, K., Harmon, R.S., 2010. TanGeoMS: Tangible geospatial modeling system. *IEEE Visualization Conference* (accepted).
- Turdukulov, U.D., Kraak, M., Blok, C.A., 2007. Designing a visual environment for exploration of time series of remote sensing data: in search for convective clouds. *Computers and Graphics* 31 (3), 370–379.
- Tuttle, B.T., Anderson, S., Huff, R., 2008. Virtual globes: an overview of their history, uses, and future challenges. *Geography Compass* 2 (5), 1478–1505.
- Underkoffler, J., Ishii, H., 1999. Urp: a luminous-tangible workbench for urban planning and design. *Proceedings of the Conference on Human Factors in Computing Systems (CHI '99)*, 15–20 May 1999, Pittsburgh, PA, USA.
- Valkov, D., Steinicke, F., Bruder, G., Hinrichs, K.H., 2010. Traveling in 3D virtual environments with foot gestures and a multi-touch enabled WIM. *Proceedings of 12th International Conference on Virtual Reality (VRIC)*, Laval, France <http://viscg.uni-muenster.de/publications/2010/VSBI10b> (accessed 7 June 2010).
- Van Aalsburg, J., Yikilmaz, M.B., Kreylos, O., Kellogg, L.H., Rundle, J.B., 2009. New frontiers in fault model visualization and interaction. *American Geophysical Union, Fall Meeting 2009* (abstract #IN43A-1137).
- Whitmeyer, S.J., De Paor, D.G., Daniels, J., Jeremy, N., Michael, R., Santangelo, 2008. A pyramid scheme for constructing geologic maps on Geobrowsers. *American Geophysical Union Fall Meeting 2008* (abstract #1140).